THE JOURNAL OF BIOLOGICAL CHEMISTRY

Vol. 268, No. 8, Issue of March 15, pp. 5711-5718, 1993
Printed in U.S.A.

# Ligand Binding and Conformation Change in the Dimeric Hemoglobin of the Clam *Scapharca inaequivalvis**

(Received for publication, October 26, 1992)

**Emilia Chiancone‡**

*From the Centro Studio sulla Biologia Molecolare, Dipartimento di Scienze Biochimiche "A. Rossi Fanelli," Università La Sapienza, Piazzale Aldo Moro 5, 00185 Roma, Italy*

**Ron Elber§**

*From the Department of Chemistry, University of Illinois at Chicago, Chicago, Illinois 60680 and the Department of Physical Chemistry and the Fritz Haber Research Center, The Hebrew University, Givat Ram, Jerusalem, 91904, Israel*

**William E. Royer, Jr.¶**

*From the Program in Molecular Medicine and Department of Biochemistry and Molecular Biology, University of Massachusetts Medical Center, Worcester, Massachusetts 01605*

**Rebecca Regan and Quentin H. Gibson‖**

*From the Department of Biochemistry, Molecular and Cell Biology, Cornell University, Ithaca, New York 14853*

**The reaction with carbon monoxide of the cooperative dimeric hemoglobin from *Scapharca inaequivalvis* has been examined by flash photolysis. In the nanosecond time range, geminate rebinding of 5% of dissociated CO occurs with a rate constant of $1.4 \times 10^7$ $s^{-1}$. There is a change in absorbance of deoxyhemoglobin following photolysis at a rate of $1.2 \times 10^6$ $s^{-1}$, consistent with a shift in the position of the Soret band to longer wavelengths. The amplitude of the change is proportional to the population of deoxydimer. In much of the Soret region this change is greater than the absorbance excursion associated with geminate recombination. There is at least one other slower change associated with the singly liganded species.**

**Geminate rebinding of NO has components of 50, 8, and 0.035 $ns^{-1}$, accounting for 75%, 25%, and less than 1% of the total reaction observed after a 35-ps photolysis flash. Simulation of diffusion of NO by molecular dynamics shows the ligands moving from the heme pocket to a subsidiary space between the edge of the heme and the surface of the protein.**

Evidence has accumulated in the last 10 years that the homodimeric hemoglobin from *Scapharca inaequivalvis* shows significant cooperativity in ligand binding (1, 2), the value of Hill's *n* reaching 1.5. A kinetic study of oxygen and carbon monoxide binding (3), which are independent of pH and salt concentration, has suggested that the mechanism of cooperativity must differ significantly from the mechanism proposed for mammalian hemoglobins by Perutz (4), and since supported by many other investigators. The 2.4-Å resolution x-ray structure for liganded *S. inaequivalvis* hemoglobin (5) has recently been supplemented by a structure for *S. inaequivalvis* deoxyhemoglobin at similar resolution (6), providing a full description of the two structures and of the changes associated with ligand binding. The helices in the subunits of *S. inaequivalvis* hemoglobin are arranged much as in myoglobin and in the subunits of mammalian hemoglobin. The subunits themselves, however, are quite differently related to one another with the E and F helices in the interface between the subunits rather than at the exterior of the molecule. In this structure, the two hemes are close together with one pair of propionate groups separated by only 4 Å (5).

The changes in conformation associated with ligand binding are also quite different, with prominent tertiary rearrangements but only subtle quaternary movements (6).

The new structural knowledge has added greatly to the interest of functional studies on the *S. inaequivalvis* protein, and, as there have been significant technical advances in kinetic methods since the original studies, a repetition and extension of the earlier kinetic work seemed appropriate. The new experiments have confirmed the older work quite satisfactorily and extend it by adding data on spectral changes in the deoxyhemes following photodissociation of CO and direct measurements of the rate of picosecond recombination of NO. The NO data fall in a range that allows molecular dynamics simulation of ligand diffusion through the protein, and the results of preliminary work are reported.

## MATERIALS AND METHODS

*S. inaequivalvis* hemoglobin was prepared as described in Ref. 3 and was preserved at liquid $N_2$ temperature until required. The buffer used was 0.1 M $KP_i$ throughout. The samples were repurified using a Pharmacia Mono Q FPLC column. Storage does not affect kinetic behavior as judged by the good reproducibility between a confirmatory set of data collected recently and corresponding data collected a year previously using the same protein sample. In addition, several partial repetitions have been made using different samples. Photolysis flashes came from a solid state laser model YG571 (Continuum Inc., Santa Clara, CA). This laser contains two oscillators, one giving mode-locked pulses of 35-ps duration, the other, Q-switched, giving pulses 9 ns long, both (after frequency doubling) at 532 nm. Data

* The costs of publication of this article were defrayed in part by the payment of page charges. This article must therefore be hereby marked "*advertisement*" in accordance with 18 U.S.C. Section 1734 solely to indicate this fact.

‡ Supported in part by Ministero della Università e Ricerca Scientifica 40% and 60% grants.

§ Supported by United States Public Health Service Grant GM-41905 and a Camille and Henry Dreyfus New Faculty Scholar and University of Illinois West Scholar.

¶ Supported by United States Public Health Service Grant DK-43323.

‖ Supported by United States Public Health Service Grant GM-14276.

deconvolution was carried out as described in Ref. 7.

A description of the apparatus used in making measurements in the millisecond time range has been given recently (7). A xenon arc and fast A/D board were used giving a small-signal response of 1 μs. Nanosecond measurements were made in real time using a photomultiplier to drive a fast oscilloscope (Tektronix 7104, Beaverton, WA). The traces were recorded with a digital camera and frame acquisition board interfaced to a microcomputer. The light source was a 75-watt xenon arc pulsed to 200 × normal brightness. Picosecond data acquisition was by a conventional pulse-probe arrangement, splitting the 35-ps pulse from the laser, using part for photolysis, and passing part through a Raman tube containing $H_2$ at 25 atmospheres pressure. The first anti-Stokes line at 436 nm was separated and used as the observation beam. The time interval was adjusted with a delay line constructed from a discarded lathe bed. Reference and observation pulses were detected with fast photodiodes used to charge a small capacitor. The voltage was read with amplifiers interfaced to an A/D board. Absorbance changes in the nanosecond time range were fitted to the scheme shown under "Discussion" by non-linear least squares and numerical integration of the corresponding differential equations. The large, relatively very slow, changes attributed to bimolecular rebinding of ligand were subtracted first. The contribution of geminate rebinding was assigned at each wavelength as a constant fraction of the amplitude associated with bimolecular rebinding. Two rate parameters remain to be assigned, one associated with the doubly unliganded form, the other with the singly liganded one. The weights given to these rates were calculated assuming a binomial distribution of unliganded, singly liganded, and doubly liganded forms of the protein after the flash. The standard errors derived from the curve-fitting procedure are unrealistically small because so many parameters have been fixed. Experience during the procedure suggests a standard error less than 20%.

Molecular dynamics simulations were carried out using the programs CHARMM (16) and MOIL.[1] The force field in MOIL is primarily a combination of AMBER (17) and OPLS (18). The improper energy terms are taken from CHARMM (19). In the locally enhanced simulation protocol correlation between ligand copies is ignored. The effect of the approximation is acceptably small when the fluctuations of the protein are weakly affected by the ligand. The two programs were used to check the sensitivity of the results to the simulation potential.

The starting point was the x-ray structure of the CO derivative of *S. inaequivalvis* hemoglobin at 2.4-Å resolution (5). After the addition of polar hydrogens and minimization (Powell, 300 steps) to remove strains, the temperature of both ligands and protein was raised to 300 K using linear scaling over 15 ps, and the simulations continued for an additional 35 ps of production run. The ligands and the protein were maintained at room temperature by velocity scaling. In the MOIL program the cutoff distance was 10 Å, with a second cutoff of 12 Å for the particle buffer. The time step was 1 fs, and the 1–4 scaling parameters were those recommended for the AMBER/OPLS combination, *i.e.* 2 and 8 for electrostatic and van der Waals, respectively. For CHARMM the 1–4 factor was 1.0 with distance-dependent dielectric, the time step was 1 fs, and the cutoff distance 10 Å. All simulations included the 214 water molecules with positions defined in the crystal structure. A total of 25 simulations were run using CHARMM and 9 with MOIL. All simulations start with the same structure, but the initial velocities were assigned randomly from the Boltzmann distribution and differ from run to run. The two programs gave generally similar results in terms of the residues closely approached by ligands.

## RESULTS

*Bimolecular and Microsecond Absorbance Changes Related to Ligand Binding*—The recent determination of the crystal structures of both liganded and unliganded forms of *S. inaequivalvis* hemoglobin has established beyond question that the structural basis of cooperativity in this protein is quite different from that of mammalian hemoglobins, as had already been suggested by earlier functional studies (1–3). The earlier kinetic studies (3) did not permit definite conclusions about the relation between absorbance changes and allosteric behavior; indeed the data showed little more than the existence of absorbance changes uncorrelated with ligand binding. They were so fast as to lie at the limit of resolution of the recording system. Both the recording system and the protein preparation have been improved since then, so, as a preliminary, all of the experiments were repeated. The results of the new and old experiments agree well.

*Oxygen Dissociation from T-state Hemoglobin*—In the earlier paper (3), this rate was calculated as the ratio of the initial rate of oxygen binding and the initial slope of the oxygen equilibrium curve, giving a rate of 580 $s^{-1}$ at pH 7.0 and 20 °C. This estimate has been supplemented by direct measurement of oxygen binding to predominantly T-state hemoglobin following flash photolysis of partially (less than 5%) saturated hemoglobin, as described by Sawicki and Gibson (8). At low saturation, most of the oxygen molecules combine with T-state hemoglobin molecules that were unliganded before the flash. Very few hemoglobin molecules have the opportunity to acquire a second oxygen molecule immediately, though they may do so as the distribution between R and T species relaxes from predominantly T-state to the ratio at equilibrium. Following the discussion of Ref. 8, the measured first-order rate closely approximates $k'_1 \cdot Hb_2 \cdot O_2 + k_1 \cdot Hb_2(O_2)$. If the experiment is performed over a range of hemoglobin concentrations, the observed rates, when plotted against hemoglobin concentration, should lie on a straight line intercepting the ordinate at $k_1$ and having a slope proportional to the rate constant for oxygen combination. An experiment of this kind gave 490 $s^{-1}$ and 11 × $10^6$ $M^{-1}$ $s^{-1}$ for on and off rates, respectively. The ratio of these rates yields the intrinsic value of the first equilibrium (dissociation) constant $K_1$ as 45 μM, in satisfactory agreement with the value of 39 μM derived by Ikeda-Saito *et al.* (9) from analysis of the oxygen equilibrium curve. The oxygen binding rate for the T-state is smaller than that for the R-state (previously reported as 15 × $10^6$ $M^{-1}$ $s^{-1}$), but the difference is not large. It is, therefore, unsurprising that no contribution to kinetic cooperativity from oxygen binding was detected in the earlier experiments that were limited to photolysis of fully liganded hemoglobin with various light intensities (3).

*Nanosecond Absorbance Changes Following Photolysis of CO-S. inaequivalvis Hemoglobin*—A half-time of 20 ns for geminate recombination of oxygen and nitric oxide was reported previously by Chiancone and Gibson (10). They were unable to obtain data for the recombination of CO because of technical limitations of their dye laser system. Measurements have now been made with a time response (to 1/e) of 1 ns.

Fig. 1 shows experimental records at 440, 437.5, and 427.5 nm after subtraction of the absorbance change corresponding to the bimolecular rebinding of CO. These rapid changes account for roughly 5% of the total absorbance change at 436 nm. At 440 nm (*panel A*) only a fast process with a half-time of ≈50 ns is apparent, whereas at the two shorter wavelengths (*panels B* and *C*) a slower process with an absorbance change of the opposite sign and a half-time of ≈0.5 μs dominates the experimental traces. The 50-ns species is attributed to the geminate rebinding of CO because: 1) the half-time is of the same order as that of the nanosecond component of the geminate reactions observed for $O_2$ and NO (10), which may be expected to follow the same pathway but at a rate limited by diffusion; 2) the amplitude is proportional to the absorbance change at 436 nm taken as a measure of photolysis; 3)

[1] The program is available via anonymous ftp from 128.248.186.70 and will be published (Elber, R., Roitberg, A., Verkhiver, G., Goldstein, R., Li, H., and Simmerling, C. (1993) *MOIL: A Molecular Dynamics Program with Emphasis on Reaction Path Calculations and Conformational Searches in Proteins* in *Advances in Computational Biology* (Villar, H., ed) Jai Press Inc., Greenwich, CT).

the kinetic difference spectrum is similar to the static difference spectrum Hb-HbCO.

The slight but significant increase in the rate of the slower process (half-time ≈0.5 μs) between 427.5 and 437.5 nm suggested there might be more than one species, and further experiments were performed with different wavelengths of observation and with partial photolysis. The data presented in Fig. 2 not only confirm the dependence of the time course on wavelength but also demonstrate the marked effect of partial photolysis in the range 430–435 nm. For these wavelengths the apparent rate is slower at the lower breakdown shown (40%). On further decrease in light intensity, reducing fractional photolysis, a distinct lag phase is apparent (Fig. 3, *main panel*). These results are dealt with more fully under "Discussion."

*Picosecond Rebinding of NO*—An example of the time course observed following a 35-ps photolysis flash is given in Fig. 4. The reaction is biphasic and was represented by a sum of exponentials. The faster component had a rate constant of 50 ± 10 $ns^{-1}$ and accounted for 0.75 ± 0.04 of the total amplitude. The second component had a rate of 7.8 ± 1 $ns^{-1}$. The effective quantum yield for NO removal, obtained by comparison with a myoglobin CO standard, was 0.6 ± 0.1. The corresponding values for sperm whale myoglobin, obtained with the same apparatus and analyzed in the same way, were 30 $ns^{-1}$, accounting for 0.79 of the observed reaction, and 4.6 $ns^{-1}$ for the slower phase of rebinding. The apparent quantum yield was 0.2. Both rates of rebinding are significantly higher in *S. inaequivalvis* hemoglobin than in sperm whale myoglobin, and the apparent quantum yield is quite unusually large when compared with reported values. This confirms by direct observation the earlier suggestion (10), based on nanosecond experiments, that the rate of recombination would be relatively high in *S. inaequivalvis* hemoglobin, but the observed value falls short of the earlier estimate of ≈100 $ns^{-1}$. This is because, at the time, it was not known that the effective quantum yield on the picosecond scale was less than 1. A corrected estimate is 60 $ns^{-1}$, much closer to the observed value.

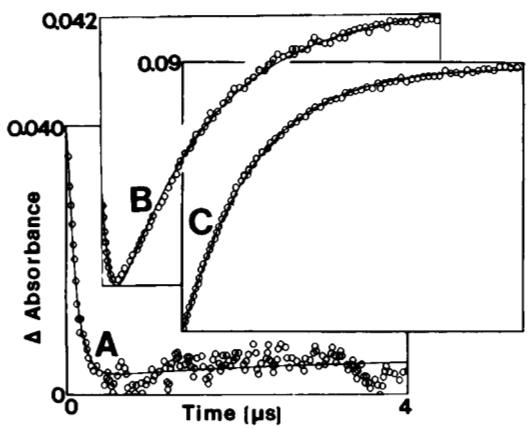


FIG. 1. **Absorbance changes following flash photolysis of 88 μM (heme) CO-*S. inaequivalvis* hemoglobin.** The path length was 1 mm, and the concentration of free CO 0.92 mM, temperature 20 °C. Photolysis was with a 9-ns flash, estimated to be approximately 32 times brighter than required for half-dissociation. Observation was at: *panel A*, 440 nm; *panel B*, 437.5 nm; and *panel C*, 427.5 nm. The total time of observation was 4 μs in each case. The absorbance values shown for each *panel* are the residuals after subtraction of the slow bimolecular contribution in each case.

## DISCUSSION

Repetition of the previous experiments (3) has given results in satisfactory agreement with the older data, and new experiments have provided a sounder base for several of the kinetic quantities. In particular, the rate of oxygen dissociation from T-state *S. inaequivalvis* hemoglobin, which previously depended on the combination of equilibrium and kinetic estimates, has been confirmed by more direct measurements at low fractional saturation. In addition, direct measurements of oxygen binding to T-state hemoglobin have shown that the allosteric change has little effect on the rate of bimolecular oxygen combination. The new experiments call for reinterpretation of the previous measurements made at the ligand binding isosbestic. This is deferred until after discussion of the new data with carbon monoxide as ligand. Its high quantum yield and modest geminate reaction allow a full range of photochemical breakdown to be examined. With oxygen, the prominent geminate reaction restricts the maximal breakdown that can be observed beyond the nanosecond range of times, and this is even more true of nitric oxide.

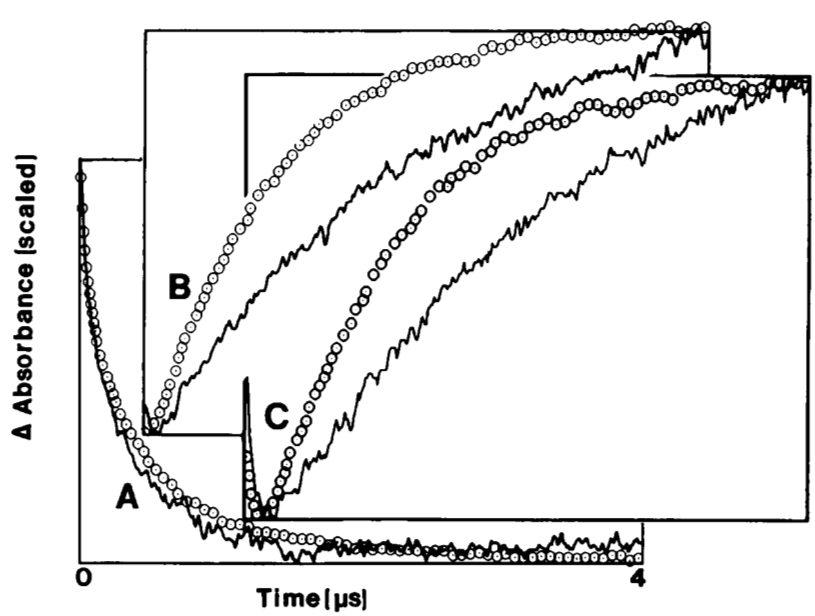


FIG. 2. **The general conditions are as for Fig. 1.** The wavelengths of observation were: *panel A*, 420 nm; *panel B*, 430 nm; and *panel C*, 435 nm. Two levels of photolysis light were used for each *panel*; the stronger flash was the same as used for Fig. 1, and the weaker 32 times less. The absorbance excursions have been normalized to emphasize the form of the time courses.

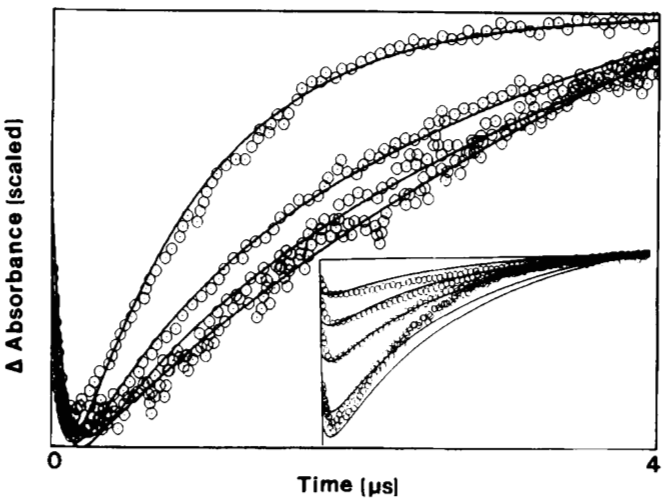


FIG. 3. **The effect of varying light intensity on the nanosecond absorbance changes measured at 435 nm.** The general conditions were as for Fig. 1. The relative intensities of the photolysis light from above downward were: 128, 64, 32, and 1, with the brightest light as in Fig. 1. The *traces* have been scaled to show the change in form. The *lines* were calculated using the scheme given under "Discussion." The values of the parameters were: $k_2 = 0.3\ \mu s^{-1}$, $k_3 = 1.2\ \mu s^{-1}$. The *inset* shows unscaled data taken from the same experiment and fitted to a single exponential (*lines*).

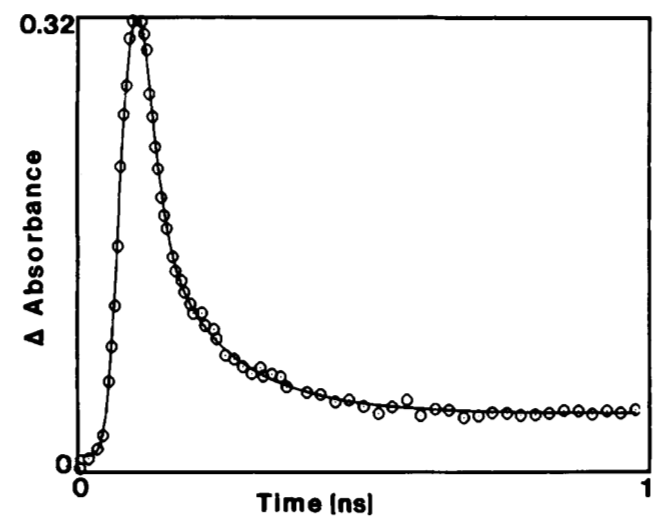


FIG. 4. **Picosecond recombination of NO to *S. inaequivalvis* hemoglobin.** The photodissociation flash at 532 nm had a width at half-height of 35 ps and a peak rate of delivery of quanta of $0.14 \times 10^{12}\ s^{-1}$. The recombination rates: $52 \times 10^9\ s^{-1}$ with a relative weight of 0.76, and $6.7 \times 10^9\ s^{-1}$, path length 1 mm, hemoglobin 65 μM in heme, temperature 22 °C, wavelength of observation 436 nm. Total time of observation was 1 ns.

The new results are quite complex. There is first, a reaction with a half-time of 50 ns attributed to geminate recombination of CO. In our experiments it accounts for from 6 to 10% of the total absorbance change with the larger proportion occurring at low fractional photolysis. This may be accounted for by recycling of ligand at high light levels during the photolysis flash lifetime of 9 ns. The first experiments, with measurements at 435 nm (Fig. 1, *panel B*) suggested that there must be at least two processes, each associated with a different absorbance change, and change of wavelength (Fig. 1, *panels A* and *C*) confirmed this supposition. Approximate difference spectra obtained by splitting the total absorbance into two components allowed the faster process (Fig. 1, *panel A*) to be assigned a rate of $1.4 \times 10^7\ s^{-1}$, somewhat lower than the geminate rebinding rate of $3.5 \times 10^7\ s^{-1}$ already reported for $O_2$ and NO (10). The difference is readily accounted for by the consideration that the observed rate constant is the sum of the rebinding rate and the rate of escape of ligand from some intermediate position in the protein. For carbon monoxide, the rate of recombination does not compete effectively with diffusion away from the protein so that the small geminate reaction monitors the escape process. With $O_2$ and NO the nanosecond rate derives roughly equally from the processes of escape of ligand from the intermediate position to the exterior and the return of ligand from the intermediate position to the heme.

Analysis of the slower component of Fig. 1 was complicated by the finding that the observed time course followed at a single wavelength was markedly dependent on the fraction photolyzed (Figs. 2 and 3). The simplest explanation, that there is more than one protein present in the samples, is difficult to rule out completely. No evidence of impurity has been found by chromatography, however, and the requirement that the faster component of the absorbance excursion shown in Fig. 2 should relate to a protein with a relatively low quantum yield excludes the possibility that it derives directly from CO-*S. inaequivalvis* hemoglobin itself, since its overall quantum yield measured on long (microsecond) time scales is close to that of sperm whale CO-myoglobin.

An alternative explanation of the effect of fractional photolysis on the data of Figs. 2 and 3 is that a conformation change takes place faster in the unliganded species than in the singly liganded one. A scheme may be written as follows.

$$\text{Light } Hb_2(CO)_2 \rightarrow Hb_2CO \rightarrow Hb_2^* \qquad \text{(Eq. 1)}$$

$$Hb_2^*CO \rightarrow Hb_2(s)CO \quad \text{rate } k_2 \qquad \text{(Eq. 2)}$$

$$Hb_2^* \rightarrow Hb_2(s) \quad \text{rate } k_3 \qquad \text{(Eq. 3)}$$

Hb(s) is written to indicate a stable species. Note that, except for the photochemical reaction (Equation 1), ligand binding is not involved. This scheme has been used to account for the data of Fig. 3. The *inset* to Fig. 3 illustrates the need for a supplementary scheme, the *lines* showing a least squares fit to the data with a single step. The body of the figure shows the fit using the scheme above with the same rates for all runs, assuming a binomial initial distribution of the intermediates in Equation 1 and taking the fractional photolysis from the amplitude of the bimolecular recombination reaction. Trials in which a separate extinction change was associated with Equation 2 did not lead to an improved fit and gave values close to zero except at wavelengths shorter than 420 nm. The amplitudes there were small, however, and the data could not be analyzed to yield two spectra reliably. A component associated with Equation 2 may, however, be responsible for the shoulder in the spectrum of Fig. 5. In preparing the figure and in other data reduction work, the difference extinction coefficient corresponding to Equation 2 was made the same as for Equation 3. The rates for Equation 3 and its extinction coefficient were obtained from experiments at high light levels where $Hb_2^*$ is the only species populated significantly. These values were used as fixed inputs in fitting the experiments at low light levels, leaving the rate for Equation 2 as the sole disposable parameter. It should be pointed out that Figs. 2 and 3 show only approximately 10% of the total absorbance excursion and that the root mean square residual for the fits of Fig. 3 was 0.0004 in absorbance, *i.e.* close to the photon noise of the system.

The operations described in the preceding paragraphs were repeated at several wavelengths to obtain the difference spectrum for Equation 3 shown in Fig. 5. As might be expected,

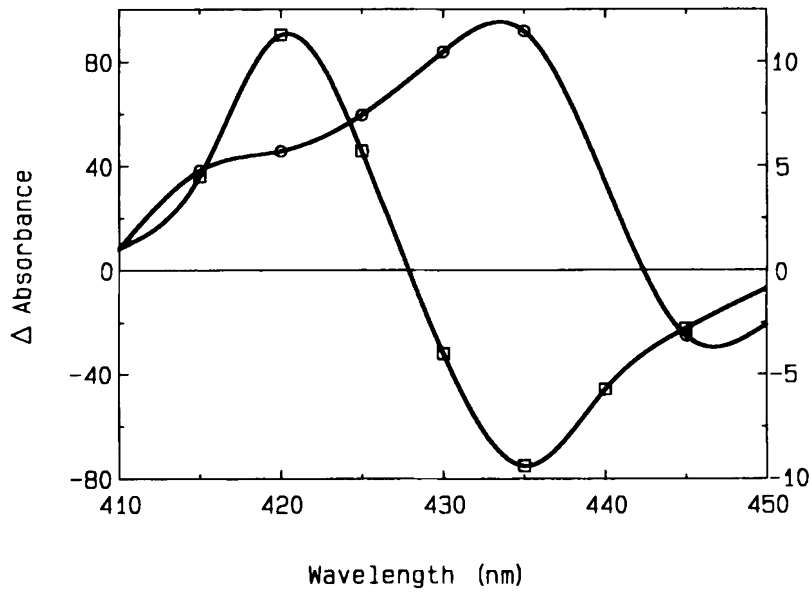


FIG. 5. **Difference spectra for binding of CO by *S. inaequivalvis* hemoglobin (□) and for the tertiary conformation change in deoxyhemoglobin (○) following photodissociation of CO.** The conditions are as for Fig. 1 for the kinetic data; the ligand rebinding spectrum was obtained by static spectrophotometry and scaled to fit conveniently within the *panel*.

this spectrum is related to the spectrum of deoxyheme rather than carbonmonoxyhemoglobin. As it passes through zero and is shifted relative to the absolute deoxy spectrum, it is reasonable to suggest that it is the expression of a small shift in the position of the deoxyhemoglobin absorption spectrum. The total amplitude is proportional to fractional photolysis, and cannot, therefore, be related to the R-T transition directly. (The extent of the R-T transition should increase more slowly than fractional photolysis at low photolysis and change more rapidly than photolysis later.) Two components are required for the analysis of Fig. 3, and the weight assigned to the faster rate ($k_3$) is proportional to the population of the deoxy dimer. If this identification is accepted, it must be supposed that the reaction represented in Figs. 2 and 3 is preceded by information transfer between deoxyhemes in the dimer in a time no longer than a few nanoseconds. This proposal may be correlated with an earlier report that the rate of the nanosecond geminate reaction with oxygen is a function of fractional photolysis (10), an observation also interpreted as evidence of intersubunit interaction on a time scale no longer than a few nanoseconds. The present results with carbon monoxide may most economically be explained by the same interaction, though this is, of course, purely speculative. Confidence in the assignment of our spectra to a conformation change is strengthened by the recent preliminary report of Ansari *et al.* (11) of analogous changes in myoglobin also attributed to conformational changes in its deoxy structure after photolysis. In *S. inaequivalvis* hemoglobin it seems that the rate of the conformational change depends on whether its partner subunit is liganded or unliganded.

The question of how these changes are related to the spectra and to the R-T transition arises immediately. In the older work (3), the R-T transition was associated with small fast absorbance changes observed at the ligand isosbestic wavelength. The existence of such changes has been confirmed, but the new finding that their amplitude is proportional to fractional breakdown means, as already stated, that they can no longer be related to the R-T transition. The original identification of the microsecond changes with the R-T transition was also consistent with their apparent reversal as small slow (millisecond) absorbance changes in the opposite direction during ligand rebinding, taken to represent the T-R

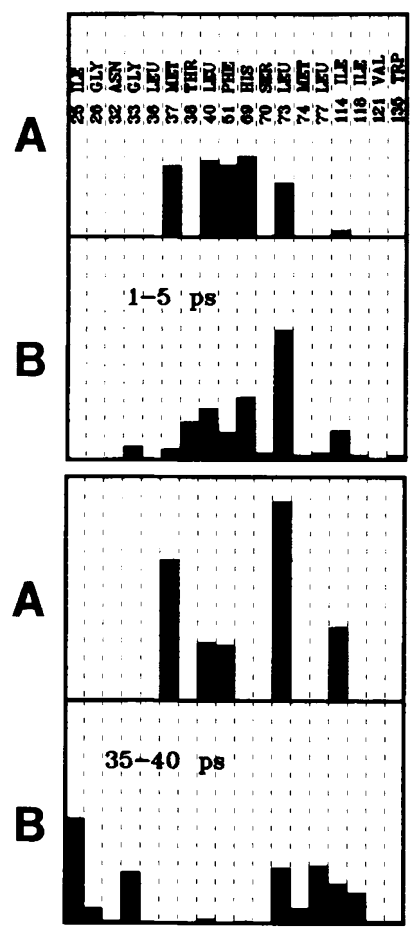


FIG. 6. **Residues closely approached (<4 Å) by ligand atoms in the simulation of diffusion in *S. inaequivalvis* hemoglobin.** The list of residues is given in the *upper part* of the *top left-hand panel*, and the relative frequencies shown by the *height* of the *bars* drawn *below* the names. In each *block* the *upper half* refers to the A heme and the *lower half* to the B heme. The interval during which the collisions were counted is shown in each *block*. The simulation used the program CHARMM as described in the text.

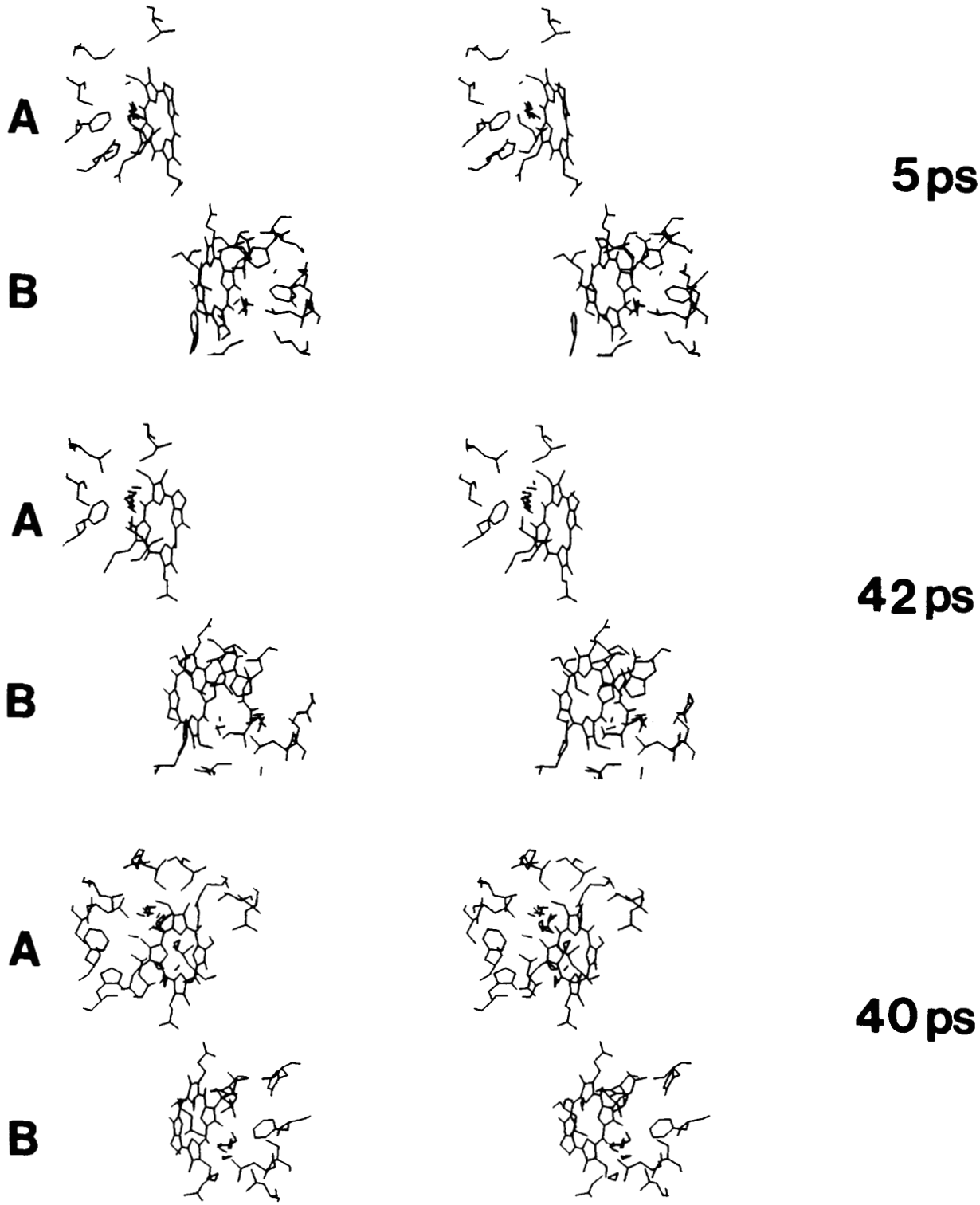


FIG. 7. **The stereo pairs show the hemes and residues closely approached by ligand atoms in molecular dynamics simulations using the CHARMM program.** The *two upper pairs* show the location of ligands in a 50-ps run in which the total number of close approaches to the iron was 297 for heme A and 13 for heme B. The times of the frames are at 5 ps and at 42 ps after initiation of the dynamics run. At 5 ps the ligands remain closely grouped and near to both A and B hemes. After 42 ps the A ligands remain close together and near heme A, while 8 of the 10 B ligands have moved away from heme B toward the viewer and form a new group with new neighbors. The *lowest stereo pair* is taken from a run with 5 approaches for heme A and 59 for heme B. In this pair water molecules appear as triangles. There are 4 molecules within the heme pocket of the A heme. The frames were taken after 40 ps.

transition (Fig. 9 of Ref. 3). This is, of course, inconsistent with the assignment of the microsecond changes as tertiary. Repetition of the millisecond experiments gave results virtually identical to those of Fig. 9 of Ref. 3, but the time courses appeared unreasonably sensitive to small changes in the monochromator setting, raising the suspicion of optical artifact. Approximate calculations using the spectra of the deoxy- and CO hemoglobins and the transmission characteristic of the monochromator were therefore performed. It was found that the calculated time course at the ligand isosbestic reproduced

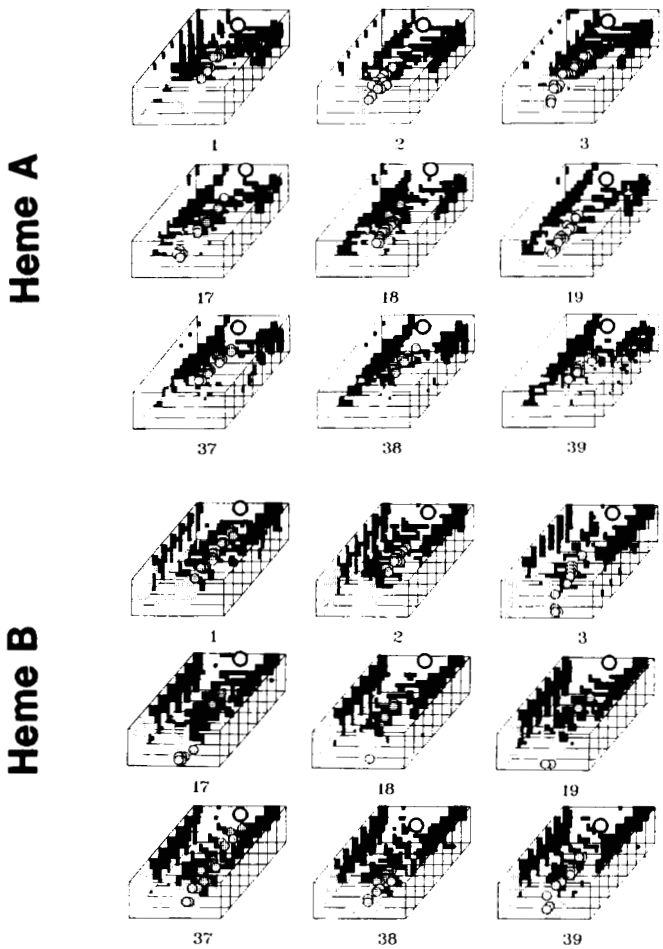


FIG. 8. **Each *block* represents the positions of the ligand copies (*small circles* with *dotted interior*), of the iron atom (*large circle* with *heavy rim*), and spaces (*shaded areas*) at the time in the simulation (ps) shown *below* the *block*.** The distances represented along the *x*, *y*, and *z* axes are 31, 11, and 8 Å, respectively. Note that the scale for the *z* axis is stretched by a factor of $3\sqrt{2}$ relative to the *x* and *y* axes. The grid slices along the *z* axis are marked at intervals of 1 Å, and the spaces for each slice are shown in progressively *less dense hatching*. The volume shown has the heme group extending across the *top*, and the *z* axis lies in the direction taken by the ligand copies in moving away from the heme iron toward the edge of the heme (see Fig. 7). During the whole period the A ligands move within the *box* while in the middle of the run the B ligands largely move out of the *box* altogether toward the observer (17–19 ps), returning later (37–39 ps).

the form and amplitude of the old and new observations admirably and that the experimental amplitude responded appropriately to change in monochromator slit width. Thus there is no longer any evidence for an absorbance change associated with the R-T transition of *S. inaequivalvis* hemoglobin. The maximum change shown in Fig. 9 of Ref. 3 was only 0.004 in absorbance, and its credibility was enhanced by comparison with analogous millisecond absorbance changes seen with tuna hemoglobin. These changes were, however, some 20 times larger than those with *S. inaequivalvis*, and their interpretation is unaffected. At present we are unable to define an optical marker relating to the R-T transition, leaving the nanosecond experiments of Ref. 10 already mentioned as the only pointer to the rate of information transfer, which would be at least 2 orders of magnitude faster than for tetrameric hemoglobins. This is consistent with the short distances and small movements of helices derived from the crystallographic studies and would seem to weight speculation toward the phenylalanine residues that both move significantly in the structure and are strategically located relative to the heme groups in the contralateral subunits (6).

Comparisons of the ligand geminate rebinding results for $O_2$, NO, and CO are consistent with their sharing a common pathway of diffusion from the heme group to the exterior (see "Results"). In the case of myoglobin, the classical pathway for ligand diffusion away from the heme group was through a gate incorporating the distal histidine (in sperm whale, residue 64) and valine 68 (12). In *S. inaequivalvis* hemoglobin the relative locations of the distal histidines (A69) and the interface are such that ligand molecules passing by them would reach the interface rather than the exterior of the protein. As a result they might remain in the protein matrix longer than would otherwise be the case, so accounting for the relatively low rates of the nanosecond geminate reactions as compared with sperm whale myoglobin (13) and leghemoglobins (14).

Molecular dynamics simulations were carried out for three reasons: 1) for comparison with recent work on mutants of sperm whale myoglobin (15); 2) to examine the pathway followed by ligands on their way toward the surface of the protein; and 3) to look for changes in the protein structure that might be related to the R-T transition. In mammalian hemoglobin there are large (7 Å) movements of substantial portions of the protein, which would not be expected to happen within the time frame of molecular dynamics calculations. *S. inaequivalvis* is quite different with the most marked changes affecting phenylalanines close to the interface and to the heme of the other dimeric subunit (6). Their movements might quite possibly occur within a time accessible to molecular dynamics simulation and, according to our current information, within 10–20 ns after dissociation of ligand (10), a time consistent with the analysis of the spectrophotometric changes studied here. In fact, no major movement of a phenylalanine was observed in a total simulation time of rather more than 1 ns, leaving the question open. The molecular dynamics simulations were carried out using a variant of the program CHARMM (16) and the program MOIL,[1] both incorporating the locally enhanced sampling method. In this approximate protocol a number of ligand copies are allowed to share a single trajectory of the protein giving a major saving in computer time. As would be expected, only a few residues were closely approached (less than 4 Å between any of the atoms of the residues and either atom of the ligands) during the first few picoseconds of simulation, and the list was the same for A and B hemes (Fig. 6). Later in the run the compact group of ligand copies may fragment, expanding the list of residues counted. This is illustrated in Fig. 6, which shows the ligands involved and the frequency of collisions for four 5-ps time periods during a simulation run. In this case the ligands associated with the B heme continued to form a compact group but have moved away from the heme.

In every case in which the ligands left the immediate area of the heme iron their movement was in the general direction illustrated in the stereo pairs of Fig. 7. In no case in which the ligands left the immediate area of the heme iron did they move past the distal histidine into the interface but instead moved away from it and from Phe A51 toward a space defined by Ile-114, Pro-117, Ile-118, and Trp-135 (all A heme numbers).

On examining the simulation results it was noticed that the ligands diffused away from the B heme more readily than from the A heme. The difference can be expressed in several ways. The number of close approaches of ligand to the heme iron was 4.4/ps for A and 1.9/ps for B in MOIL runs, and 2.5/ps and 1.2/ps in CHARMM runs giving ratios of 2.3 and

2.1, respectively (see also Fig. 6). The same pattern appears in the totals for all approaches to the heme group where the corresponding numbers were 66/ps for A and 44/ps for B (MOIL), and 35/ps and 22/ps (CHARMM) giving ratios of 1.5 and 1.6, respectively. The wider spreading out of the ligands in the B hemes was also evident in the numbers of residues accumulating more than 10 near approaches, with an average of 7 residues in the list for the A heme and 11 for the B heme. The difference between the A and B subunits is due to slight differences in the placement of hydrogens and subsequent minimization, and the overall result may be regarded as averaging two different spatial initial conditions. They cannot reflect real differences between the chemically identical subunits.

The differences between the subunits are minor when compared with the effect of altering the initial distribution of velocities assigned randomly at the beginning of the dynamics run. In the MOIL runs the largest and smallest numbers of close approaches to the heme iron were 1024 and 22 for the A heme and 649 and 0 for the B heme in 60 ps. In the CHARMM runs the corresponding counts were 308 and 4 for the A heme and 261 and 13 for the B heme for 50 ps. These large differences are similar to those reported for several mutants at position B10 of sperm whale myoglobin (15) and support the conclusion that quite small initial differences may produce effects lasting for many picoseconds.

The two molecular dynamics programs, which are differently parameterized, have shown relatively small divergences in their results. The largest quantitative difference between them was in the behavior of the water molecules, which, with CHARMM, had many encounters with ligands and sometimes moved into the space near the heme iron after the ligands had moved away, as illustrated in Fig. 7. With MOIL there were frequently no encounters between ligands and water, and no more than two water molecules had such collisions in any one run.

Comparison of the simulations of *S. inaequivalvis* hemoglobin with recent simulations of sperm whale myoglobin (15) shows that although the ligands remain in a compact group in many simulations in both proteins, in *S. inaequivalvis* there is a much greater probability of their moving further away from the heme.

This is illustrated in Fig. 8, which shows the spaces and ligand positions in a volume 30 × 11 × 7 Å in $x$, $y$, and $z$, respectively. The heme group is in the floor of the *boxes*, and the two heme groups, which were taken from the same simulation run, have been rotated into the same attitude. Examination of the diagrams shows that in both A and B hemes the ligands move away from the iron toward the front of the *boxes*, occupying all the space available to them. In the B heme larger movements occur, and most of the ligands move out of the box altogether after a few picoseconds, returning later. In both cases return to the iron is prevented much of the time with no clear path open to the ligands. Although this is consistent with the experimental finding that NO molecules that do not rebind on a picosecond scale take part in a relatively slow geminate reaction, a causal relation is far from being established. The molecular dynamics observations offer, for the future, suggestions for site-directed mutagenesis and a prediction of a possible xenon binding site beyond the edge of the heme group which may be demonstrable by x-ray crystallography.

REFERENCES


1. Chiancone, E., Vecchini, P., Verzili, D., Ascoli, F., and Antonini, E. (1981) *J. Mol. Biol.* **152,** 577–592
2. Antonini, E., Chiancone, E., and Ascoli, F. (1982) in *Structure and Function Relationships in Biochemical Systems* (Bossa, F., Chiancone, E., Finazzi-Agro, A., and Strom, R., eds) pp. 67–73, Plenum Publishing Corp., New York
3. Antonini, E., Ascoli, F., Brunori, E., Chiancone, E., Verzili, D., Morris, R. J., and Gibson, Q. H. (1984) *J. Biol. Chem.* **259,** 6730–6738
4. Perutz, M. F. (1979) *Annu. Rev. Biochem.* **48,** 327–386
5. Royer, W. E., Jr., Hendrickson, W. A., and Chiancone, E. (1989) *J. Biol. Chem.* **264,** 21052–21061
6. Royer, W. E., Jr., Hendrickson, W. E., and Chiancone, E. (1990) *Science* **249,** 518–521
7. Bellelli, A., Blackmore, R. S., and Gibson, Q. H. (1990) *J. Biol. Chem.* **265,** 13595–13600
8. Sawicki, C. A., and Gibson Q. H. (1977) *J. Biol. Chem.* **252,** 7538–7547
9. Ikeda-Saito, M., Yonetani, T., Chiancone, E., Ascoli, F., Verzili, F., and Antonini, E. (1983) *J. Mol. Biol.* **170,** 1009–1018
10. Chiancone, E., and Gibson, Q. H. (1989) *J. Biol. Chem.* **264,** 21062–21065
11. Ansari, A., Jones, C. M., Henry, E. R., Hofrichter, J., and Eaton, W. J. (1992) *Science* **256,** 1796–1798
12. Case, D. A., and Karplus, M. (1979) *J. Mol. Biol.* **132,** 343–368
13. Petrich, J. W., Poyart, C., and Martin, J. L. (1988) *Biochemistry* **27,** 4049–4060
14. Gibson, Q. H., Wittenberg, J. B., Wittenberg, B. A., Bogusz, D., and Appleby, C. A. (1989) *J. Biol. Chem.* **264,** 100–107
15. Gibson, Q. H., Regan, R., Elber, R., Olson, J. S., and Carver, T. E. (1992) *J. Biol. Chem.* **267,** 22022–22034
16. Elber, R., and Karplus, M. (1990) *J. Am. Chem. Soc.* **112,** 9161–9175
17. Weiner, S. J., Kollman, P. A., Case, D. A., Singh, U. C., Ghio, C., Alagona, S., Porfeta, S., and Weiner, P. (1980) *J. Am. Chem. Soc.* **106,** 765–784
18. Jorgensen, W. L., and Tirado-Rives, J. (1988) *J. Am. Chem. Soc.* **110,** 1657–1666
19. Brooks, B. R., Bruccoleri, R. E., Olafson, B. D., States, D. J., Swaminathan, S., and Karplus, M. (1983) *J. Comput. Chem.* **4,** 187–217